Available online at www.sciencedirect.com
ScienceDirect
Journal of Power Sources 176 (2008) 215–221
JOURNAL OF POWER SOURCES
www.elsevier.com/locate/jpowsour

Effect of heat treatment and chemical composition on the corrosion behavior of Ni–Al intermetallics in molten (Li + K) carbonate

J.G. Gonzalez-Rodriguez [a,*], E. Mejia [a], I. Rosales [a], V.M. Salinas-Bravo [b], G. Rosas [c], A. MArtinez-Villafañe [d]

[a] *Universidad Autonoma del Estado de Morelos, CIICAp, Av. Universidad 1001, Col. Chamilpa, 62209-Cuernavaca, Mor., Mexico*
[b] *Instituto de Inv. Electricas, Gerencia de Procesos Termicos, Reforma 108, Temixco, Mor., Mexico*
[c] *Universidad Michoacana de San Nicolas de Hidalgo, Instituto de Inv. Metalurgicas, Morelia, Mich., Mexico*
[d] *CIMAV-Miguel Cervantes 120, Complejo Ind. Chihuahua, Chih., Mexico*

Received 30 August 2007; received in revised form 17 October 2007; accepted 18 October 2007
Available online 23 October 2007

Abstract

The corrosion performance of several Ni–Al alloys in 62 mol% Li_2CO_3–38 mol% K_2CO_3 at 650 °C has been studied using the weight loss technique. Alloys included 50Ni–50Al at.% (NiAl) and 75Ni–25Al at.% (Ni_3Al) alloys with additions of 1, 3 and 5 at.% Li each one, with or without a heat treatment at 400 °C during 144 h. For comparison, AISI-316L type stainless steel was also studied. The tests were complemented by X-ray diffraction, scanning electronic microscopy and micro-analyses. Results showed that NiAl-base alloy without heat treatment presented the lowest corrosion rate even lower than Ni_3Al alloy but still higher than conventional 316L-type stainless steel. In general terms, by either by heat treating these base alloys or by adding Li, the mass loss was increased. This effect was produced because by adding Li the adhesion of the external protective layer was decreased by inducing a higher number of discontinuities inside the grain boundaries. When the alloys were thermally annealed, these irregularities in the grain boundaries disappeared, decreasing the number of paths for the outwards diffusion of Al from the alloy to form the external, protective Al_2O_3 layer.

Keywords: Molten carbonate corrosion; Fuel cells; Ni–Al intermetallics; Heat treatment

1. Introduction

Molten carbonate fuel cells (MCFC) are energy conversion devices that directly convert chemical energy in fossil fuels into electricity. MCFCs operate in molten carbonate $(Li,K)_2CO_3$ electrolyte at about 650 °C and consist of several cells composed of absorbent, lithiated NiO cathode, $LiAlO_2$ ceramic matrix and absorbent Ni anode connected by stainless-steel separator plates. The severe corrosion of stainless steel when is used as a separator material is well known [1,2] and is one of the main problems to be resolved for the commercialization of MCFC's. Indeed, the corrosion of the wet-seal of the separator is the most serious problem for achieving maintenance-free operation for 40,000 h approximately.

NiAl and Ni_3Al intermetallics are used as high-temperature aerospace materials, and several other applications have been found due to their high-melting point (1395–1638 °C), low density and excellent thermal conductivity. NiAl forms NiO which dissolves in molten carbonate and causes reduction of the current density by electrical discharge when corrosion continues in molten carbonate. This has been noted as one of the main factors that reduce the cell output [3] energy. Indacochea et al. [4] used stainless steel such as AISI-316L or 310S but found some problems such as changes in the stainless-steel structure due to the high-annealing temperature (above 1000 °C). Murai et al. [5] used Al–Ni plated material and reported to provide longer lifetime than Al-plated material. For a large amount of Al in Al–Ni plated materials, Al is retained as an Al–Ni intermetallic compound under the $LiAlO_2$ layer. On the contrary, the Al in Al–Ni plated material tends to diffuse from the surface into the substrate. NiAl is the main compound of the Al–Ni plated coating and provides a sufficient source of Al to the

* Corresponding author.
E-mail address: ggonzalez@uaem.mx (J.G. Gonzalez-Rodriguez).

0378-7753/$ – see front matter © 2007 Elsevier B.V. All rights reserved.
doi:10.1016/j.jpowsour.2007.10.045

$LiAlO_2$ layer, which is the stable form of alumina (Al_2O_3) in molten Li/K carbonate. Pérez et al. [6] evaluated the behavior of the Al coated AISI-310S type stainless steel by the slurry method in an ion vapor deposition (IVD) in molten carbonate at 650 °C. Their characterization has shown the presence of $LiAlO_2$ coating, that allowed an important increment of the steel lifetime in molten carbonate. Agüero et al. [7] deposited FeCrAl and NiAl on t AISI-310 type stainless-steel surface by using the thermal spray coatings method and tested by immersion in a molten carbonate eutectic mixture at 700 °C. Their results indicate that the FeCrAl coating exhibited a higher molten salt corrosion resistance than IVD aluminum coatings, whereas the NiAl was damaged shortly after the beginning of the test. Escudero et al. [8] evaluated lithium–nickel mixed oxides with high-lithium content ($Li_xNi_{1-x}O$, $x = 0.30$–0.40) in an eutectic melting $(Li,K)CO_3$ at 650 °C, and the results showed that Li–Ni oxides samples reduced the nickel dissolution in the eutectic in one order of magnitude compared to the NiO.

Ni–Al type intermetallics are widely used due to their high-temperature oxidation resistance and their ability to develop an Al_2O_3 protective layer which also provides corrosion resistance in molten salts [9,10]. However, one of the main problems for these aluminides is their poor ductility. Salazar et al. [11] found that by alloying with Li results in the improvement of their ductility measuring their compressive ductility, and this improvement was increased when the specimens were annealed at 400 °C during 120 h. Thus, the aim of this work is to evaluate the effect of small additions of Li on the corrosion resistance of Ni–Al intermetallics in molten $(Li,K)_2CO_3$ at 650 °C with heat treatment and compare them with an AISI-316L type stainless steel, commonly used in bipolar plates in MCFCs.

2. Experimental procedure

Intermetallic 50Ni–50Al at.% (NiAl) and 75Ni–25Al at.% (Ni_3Al) alloys were melted in an induction furnace using stainless-steel crucibles. Pure Li with 1, 3 and 5 at.%, respectively, were added to the Ni–Al intermetallic compounds. All elements were 99.9% of purity. In order to avoid the specimens machining procedure the ingots were obtained with final dimensions according to the E800b ASTM standard. Cylindrical specimens dimensions were 1.2 cm diameter × 4.5 cm length in the test section and 5.0 cm for the final section. The ingots were homogenized to minimize the thermal vacancy effects by heat treating (HT) at 400 °C during 120 h under an argon atmosphere. The corrosive salts used in the tests were synthetic potassium carbonate (K_2CO_3) and pure lithium carbonate (Li_2CO_3) with the composition 62 mol% Li_2CO_3–38 mol% K_2CO_3 at 650 °C. All the reagents were analytical grade. Before corrosion tests the specimens (30 mm × 20 mm × 1 mm) were cleaned with acetone and dried with hot air, and finally packed in the mixture of salts in porcelain crucibles with 500 mg cm^{-2} of the synthetic salt. The corrosion tests were carried out into an electric furnaces in a static air during 100 h. After the corrosion tests, the corrosion rate was measured as weight loss. Three specimens of each condition test were decaled and chemically cleaned according to ASTM G1 81 standard: all the specimens, including 316L type stainless steel, were immersed in ammonium citrate, in a concentration of 200 g l^{-2} at 80 °C, several times until no more weight loss was detected. One of each specimens was mounted in bakelite in a cross-section and polished to analyze the subsurface corrosive attack using a scanning electron microscopy (SEM) equipped with energy dispersive spectroscopy (EDX) system to carry out chemical analyses. Finally, the corrosion products of some specimens were analyzed in a Phillips X-ray diffractometer.

3. Results and discussion

Fig. 1 shows the microstructure of NiAl-base alloys, where it is observed the presence of a great amount of small particles (sub-grains) of 20 μm approximately on the surface sample that partially disappeared for the heat treated specimens (Fig. 1b). In Fig. 1b it is observed the presence of almost a single-phase structure with a remarked misorientation between the grains, which is in good agreement with the phase diagram. Fig. 1c and d show the surface image of the samples with 5Li at.%, showing a recrystallized structure and specifically in Fig. 1d, for the annealed specimen, it is observed a clear sub nucleation inside the grain, which produced a great amount of small sub-grains and, thus, a higher surface area, correlated with a larger grain boundaries and the generation of a coarser structure. On the other hand, Fig. 2a and b present the microstructure of the Ni_3Al alloys with no Li additions in the as-cast and annealed conditions, respectively. It is clear the presence of interdendritic space (dark zone) which corresponds to a NiAl cubic B2-crystal structure due to the presence of less area fraction, while the dendritic zone is a Ni_3Al cubic $L1_2$ crystal structure. Between these two samples there is not a remarkable difference on morphology, only a partial reorientation of the grains, as observed in Fig. 2b. In Fig. 2c and d a change on the surface of the samples which contain 5 at.% of Li can be observed, mainly in the formation of sub-grains inside the interdendritic space, a coarser structure in comparison with the sample without Li, and this nucleation inside the grains presumably is produced by the addition of Li.

Fig. 3 shows the mass loss of the different materials, without heat treatment, after exposure into a molten $(Li,K)_2CO_3$ deposit during 100 h at 650 °C, whereas the results for the heat treated alloys are given in Fig. 4. It can be seen that the NiAl-base alloy without heat treatment suffers the lowest mass loss, but still higher than that for 316L stainless steel for about one order of magnitude. In the case of NiAl without heat treatment, the higher the Li contents, the greater the mass loss. The corrosion rate for Ni_3Al alloy was one order of magnitude higher than that for NiAl alloy, and for this reason it is established that the addition of 1 and 5% Li decreased this corrosion rate, whereas the addition of 3% Li increased it. When the alloys were heat treated, all the alloys had a similar mass loss, but the NiAl alloy still with the lowest corrosion rate, one order of magnitude higher than the same alloy without heat treatment. Concluding, in the case of annealed specimens, we can say that, regardless the Li contents, the alloys showed very similar corrosion rates.

SEM micrograph of the NiAl-base alloy without heat treatment is given in Fig. 5, showing the corrosion products layer. A

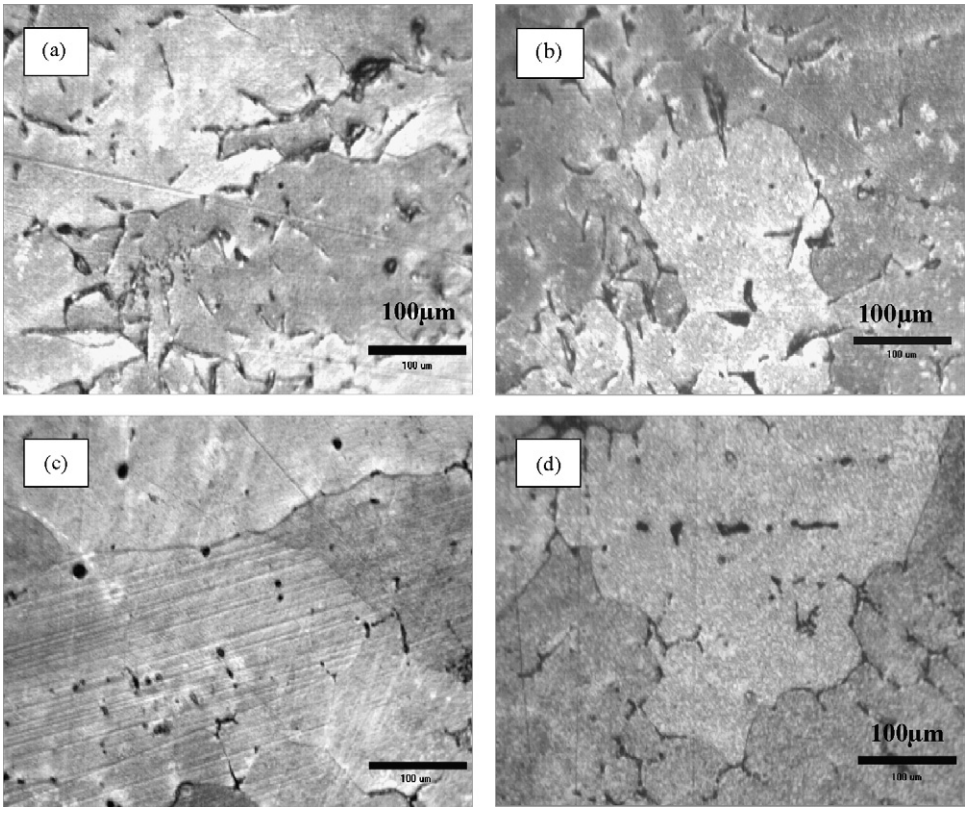

Fig. 1. Microstructures of the NiAl alloy observing in (a) as cast sample, with no Li additions; (b) annealed sample with no Li additions; (c) sample with 5% Li without heat treatment; and (d) sample with 5% Li and with heat treatment.

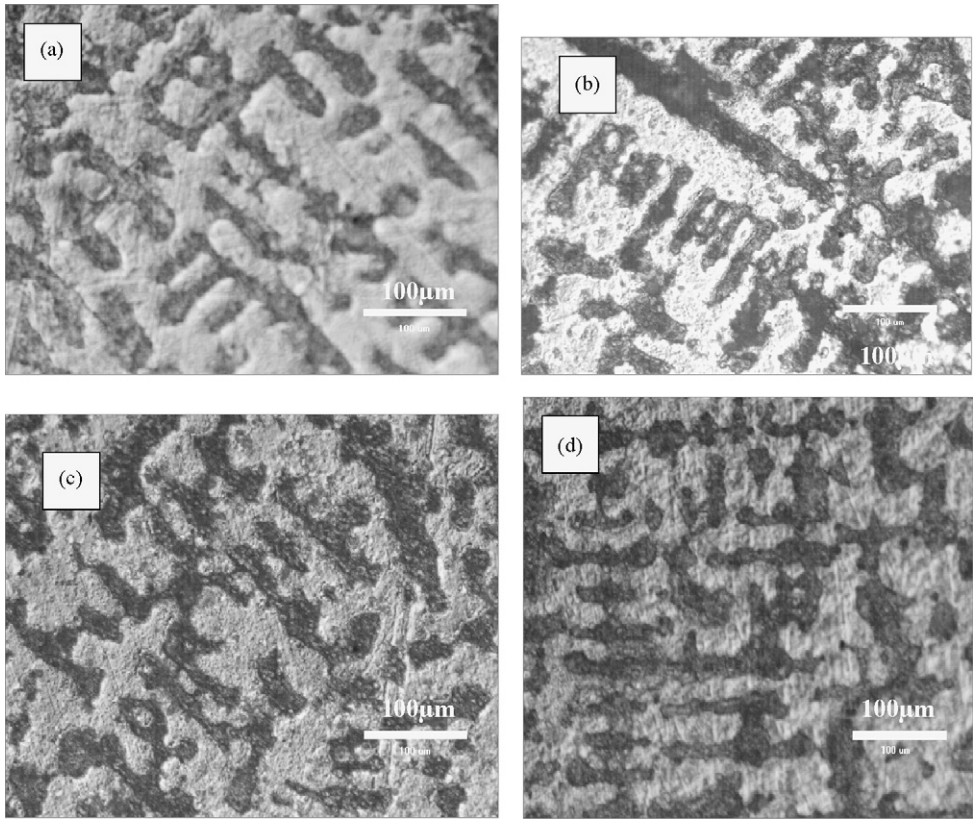

Fig. 2. Microstructures of the Ni_3Al alloys observing in (a) as cast sample with no Li additions; (b) annealed sample with no Li additions; (c) sample without heat treatment with 5% Li; and (d) annealed sample with 5% Li.

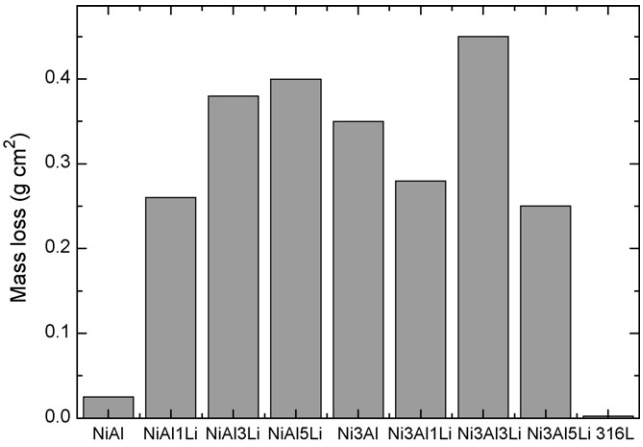

Fig. 3. Weight loss of NiAl and Ni_3Al intermetallic alloys in molten $(Li,K)_2CO_3$ at 650 °C during 100 H.

localized type of corrosion, pits-like, can be seen on the metal surface, EDX analysis performed inside of these pits show that the corrosion products were made mainly of Ni, Al, Fe and K. Since we are using high-purity NiAl alloys, the detected Fe must come from the crucible (which was made of stainless steel). The X-ray diffraction pattern, shown in Fig. 6, reveals the presence of the NiAl aluminide phase together with $LiKCO_2$, K_2CO_3, the salt components, NiO, but it is notorious the presence of the $LiAlO_2$ oxide. $LiAlO_2$ has been reported to give some corrosion protection in molten carbonate mixtures [12–14] It was not detected the presence of a protective Al_2O_3 which maybe was absorbed by the eutectic $(Li,K)_2CO_3$ deposit, and it was transformed in to $LiAlO_2$.

SEM image of the corroded NiAl alloy surface containing 3Li (at.%) is shown in Fig. 7 together with the EDX analysis of the corrosion products on the metal/deposit interface. This images revealed the presence of localized type of corrosion, as pitting damage, whereas a micro-chemical analysis inside these pits revealed the presence of Al, Ni, Fe and K. Once again, Fe must come from the stainless-steel crucible. The corrosion products consisted, again, of $LiKCO_2$, K_2CO_3, NiO and $LiAlO_2$ oxides, as can be seen in Fig. 8.

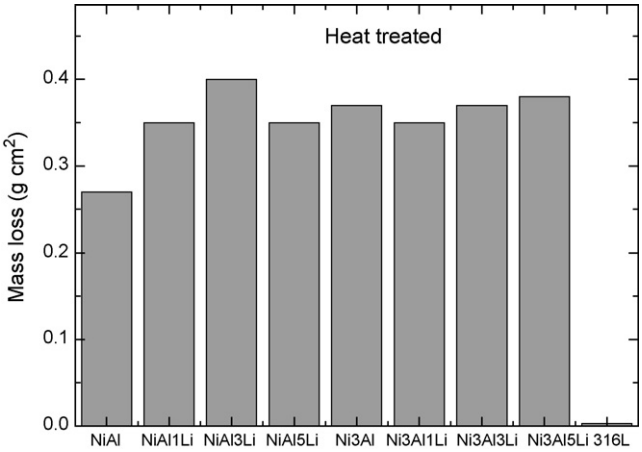

Fig. 4. Weight loss of heat treated NiAl and Ni_3Al intermetallic in molten $(Li,K)_2CO_3$ at 650 °C during 100 H.

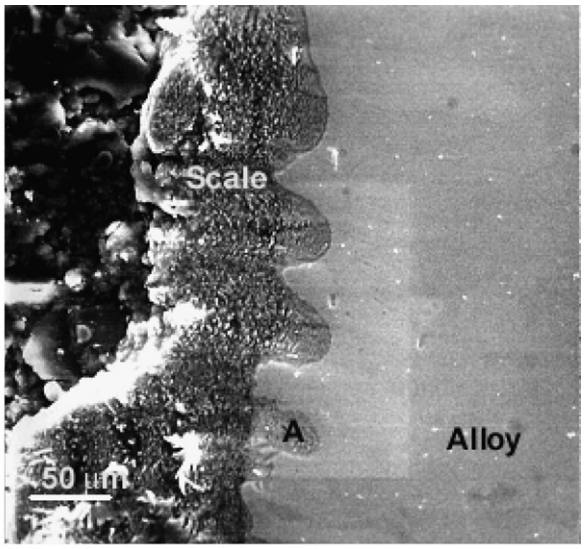

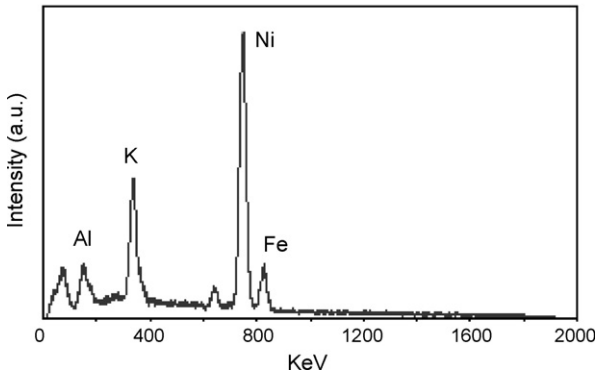

Fig. 5. Micrograph of NiAl specimen corroded in molten $(Li,K)_2CO_3$ at 650 °C together with an EDX analysis of the corrosion products in point A.

A cross-section of the corroded surface for heat treated alloy containing 3Li (at.%) is presented in Fig. 9 together with the X-ray mappings of Al, O and C. This figure shows the presence of C, O and some Al. In this case, the presence of these chemical elements at the same points may indicate that the salt components $(Li,K)CO_3$ have dissolved the protective Al_2O_3 layer. The

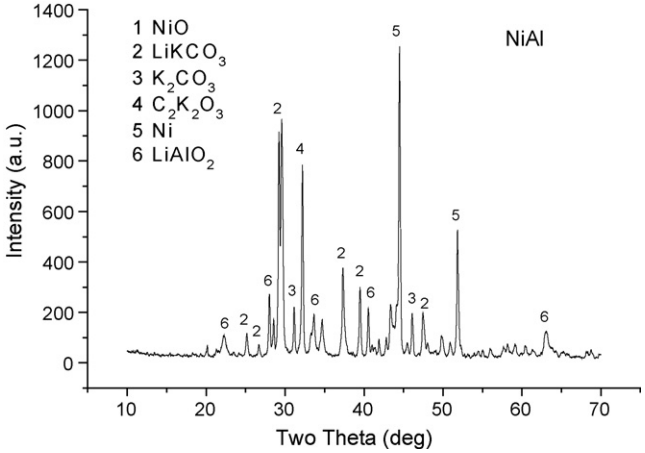

Fig. 6. X-ray diffractogram showing the corrosion products found on the NiAl-base alloy.

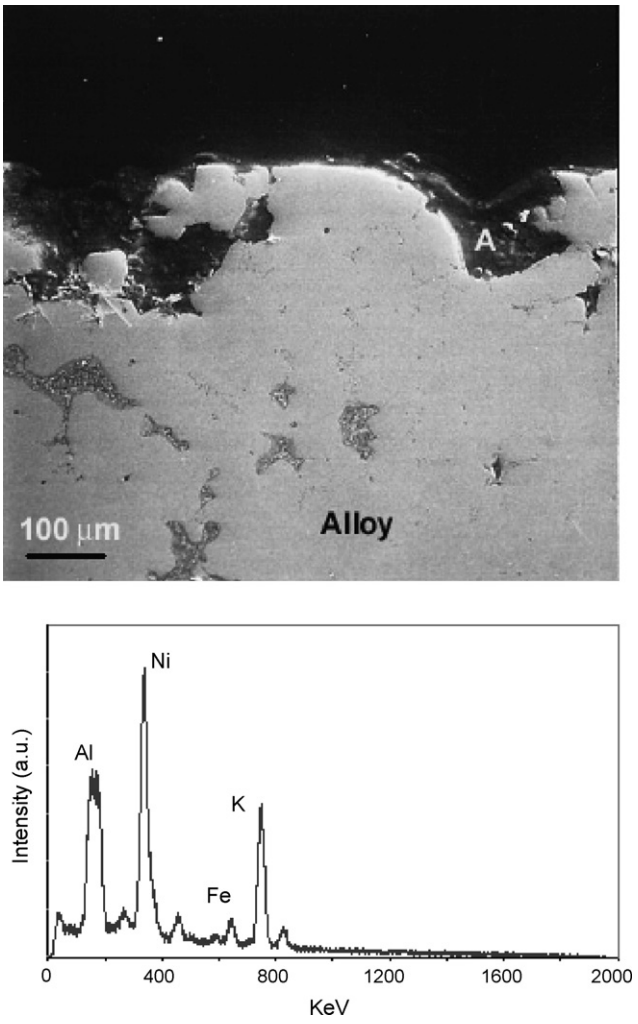

Fig. 7. Micrograph of NiAl + 3%Li in molten $(Li,K)_2CO_3$ at 650 °C together with an EDX analysis of zone A.

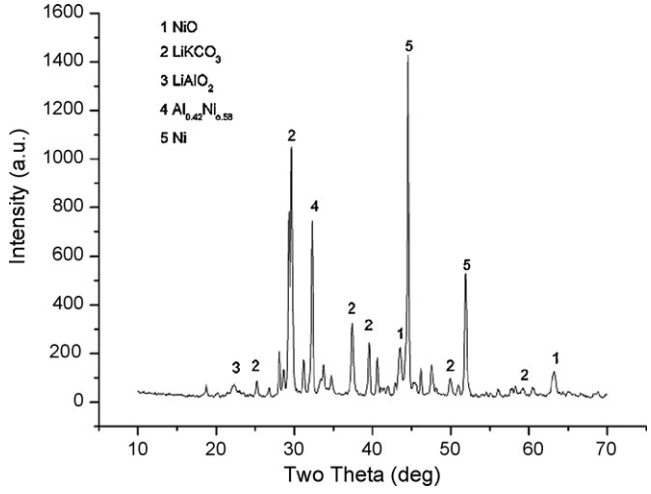

Fig. 8. X-ray diffractogram showing the corrosion products found on the NiAl + 3Li alloy.

XRD analysis of the corrosion products consisted of the same phases found in the former specimens, i.e. $LiKCO_2$, K_2CO_3, NiO and $LiAlO_2$ oxides.

For the Ni_3Al alloys the SEM and X-ray studies revealed that the precipitated oxides were not very different in comparison with those found in the NiAl alloys, regardless the heat treatment, as is evidenced in Fig. 10. This figure shows that the corrosion products consisted of Al, O and C, indicating that the external protective Al_2O_3 layer perhaps had been dissolved by the molten $(Li,K)CO_3$, whereas the X-ray analysis revealed the presence of the same compounds as those found in the NiAl-base intermetallics, i.e. $LiKCO_2$, K_2CO_3, NiO and $LiAlO_2$ oxides.

Nishina and Uchida [15] have shown that the first stage of the reduction of the O_2 in the molten carbonate resulted in a CO_2 production with the reaction:

$$2CO_3^{2-} \rightarrow 2O^{2-} + 2CO_2 \quad (1)$$

$$O_2 + 2CO_3^{2-} \rightarrow 2O_2^{2-} + 2CO_2 \quad (2)$$

These reactions are governed by the acidity of the melt (in the less acidic melts which correspond to our conditions), the reaction in Eq. (2) prevails, including a more important CO_2 formation in the melt. In the case of immersion of Al-rich alloys in molten carbonate, the following electrochemical reactions would take place:

$$Al \rightarrow Al^{3+} + 3e^{-} \text{ to form } Al_2O_3 \text{ and } LiAlO_2 \quad (3)$$

$$Fe \rightarrow Fe^{3+} + 3e^{-} \text{ to form } Fe_2O_3 \text{ and } LiFeO_2 \quad (4)$$

$$O_2^{2-} + 2e^{-} \rightarrow 2O^{2-} \text{ to form reactions (2)–(4)} \quad (5)$$

$$Ni \rightarrow Ni^{2+} + 2e^{-} \text{ to form } NiO(Fe, Ni)Al_2O_4 \quad (6)$$

These corrosion products were detected by EDX (Figs. 5 and 7) and by XRD analysis (Figs. 6 and 8). In a similar way to Al and Fe, chromium present in 316L type stainless steel must form a chromium oxide, Cr_2O_3, and then react with Li to form a compound such as $LiCrO_2$, giving corrosion protection to the steel. This could explain the low corrosion rate for AISI-316L stainless steel reported in Figs. 3 and 4. The corrosion protection of an alloy against salt melt attack depends on the chemical stability of both the kind of metal and their compounds such as oxides, carbonates, etc. In fact, a breakdown of the protective oxide scale occurs by dissolution into the melt, and the degradation rate can be specially fast if the oxide has a high solubility. With the formation of the Al_2O_3 layer, the corrosion rate decreases. The predominant surface product that forms between 600 and 800 °C has been reported to be α-Al_2O_3 [16], but it is quite possible for γ-Al_2O_3 or θ-Al_2O_3 to exist in this temperature range [17]. These forms of alumina are faster growing, more voluminous, more porous and less protective than α-Al_2O_3 [18]. The temperature at which a transition from other types of alumina to the slower growing α-Al_2O_3 appears to be 900 °C [18]. In the NiAl-base alloy, the alumina whisker cannot form a protective layer, which cannot provide an effective barrier to stop the diffusion of Ni and the diffusion to the interface of the oxygen, and this can be seen on the results obtained by the NiAl alloy which is

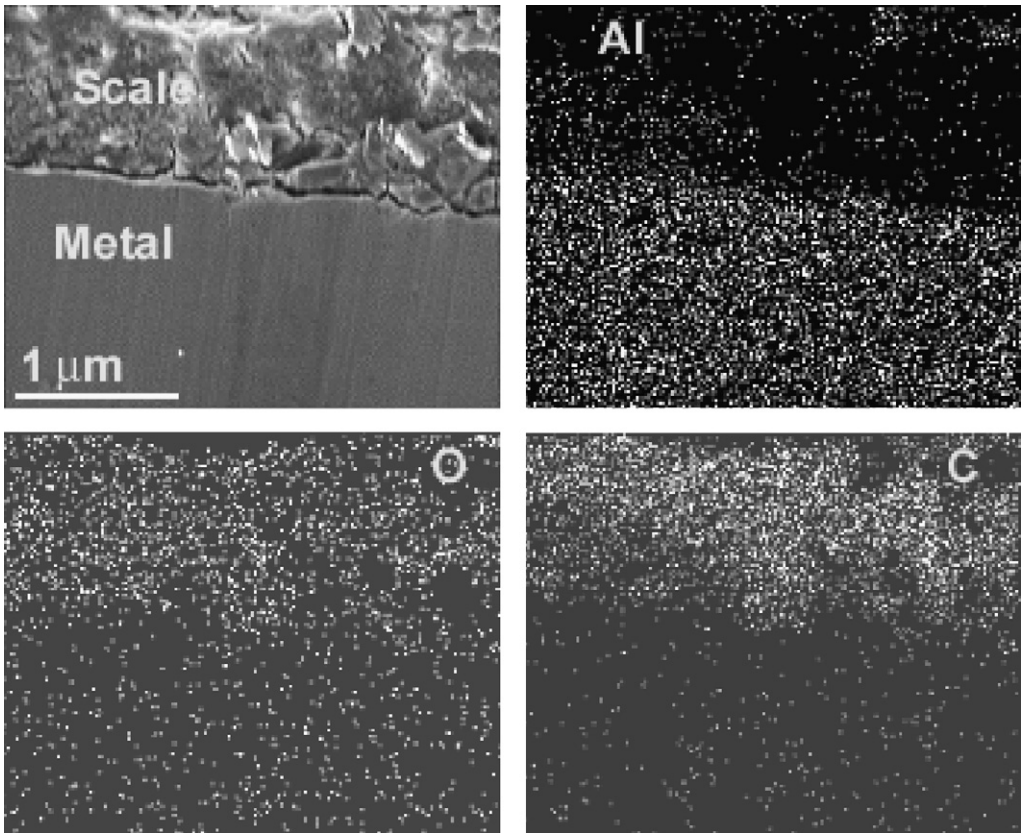

Fig. 9. Micrograph of NiAl {3%Li} with heat treatment in molten $(Li,K)_2CO_3$ at 650 °C during 100 H together with X-ray mappings of Al, O and C.

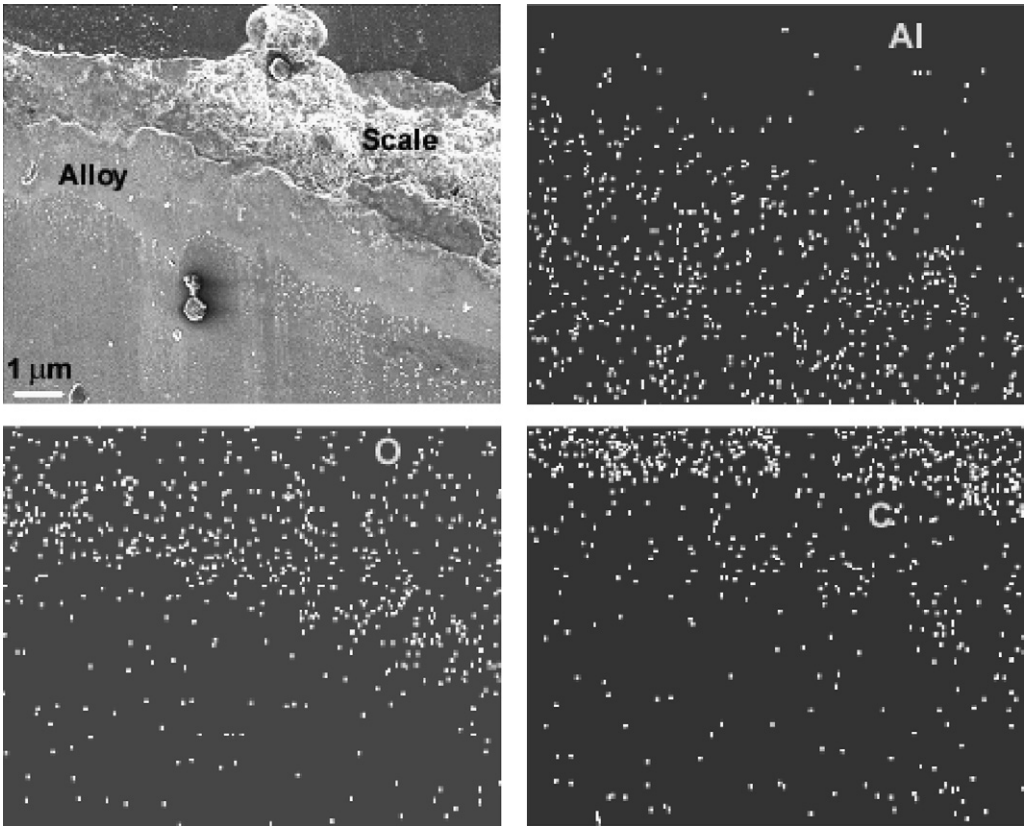

Fig. 10. Micrograph of $Ni_3Al + 3\%Li$ with in molten $(Li,K)_2CO_3$ at 650 °C together with X-ray mappings of Al, O and C.

higher than those obtained by the rest of the alloys. On the other hand, the formation of Al_2O_3 consumes certain quantity of Al, reducing its activity and partial pressure of the oxygen. This produces a relative increment in the activities of the Ni to react with the molten mixture and to obtain compound such as $NiO(Fe,Ni)Al_2O_4$.

Frangini and Masci [19] has demonstrated that additions of some ternary elements to NiAl intermetallics such as Cr or Ti improve the Al_2O_3 protectiveness by suppressing the spalling of these scales. The higher the contents of Al, the higher the corrosion resistance, so this explains why NiAl has a higher corrosion resistance then N_3Al intermetallics. Figs. 1 and 2 showed that additions of Li lead to the formation of a great amount of small sub-grains and, thus, a higher surface area, correlated with a larger grain boundaries. The adhesion of the protective Al_2O_3 depends, upon some other factors, on the number of grain boundaries, since they represent discontinuities on the metal surface, which make the film less stable, since these discontinuities represent points for a weak adhesion of the scale. This explains why, in general terms, an increment in the Li contents brings an increase in the corrosion rate. On the other hand, Fig. 1a and b, respectively, showed that by annealing the NiAl alloy the sub-grains present in the specimen without heat treatment disappeared, bringing a decrement in the number of paths for the outwards diffusion of the Al present in the alloy to form the external, protective Al_2O_3 layer, leading to a decrease the corrosion rate when the alloy was annealed. This thermal annealing did not have the same effect on the N_3Al intermetallic, since the morphologies for both specimen with and without thermal annealing are practically the same (Fig. 2a and b), so the corrosion rate was very similar for both specimens. Scale cracking, spalling or dissolution in a melt, makes the layer less protective and, thus, the corrosion rate is increased. Additionally to the dissolution of the protective scales, the dissociation of the $(Li,K)CO_3$ allowed the diffusion of Li and K, and a consequent increment of these elements on the metal/scale interface. This caused the detachment and cracking of the protective scale, allowing the corrosion of the material.

4. Conclusions

A study on the effect of heat treatment and additions of 1, 3 or 5 at.% of Li on the corrosion performance of N_3Al and NAl intermetallic alloy in molten 62 mol%Li_2CO_3–38 mol%K_2CO_3 at 650 °C has been carried out using the weight loss technique. Results showed that the NiAl-base alloy showed the lowest degradation rate, in comparison with Ni_3Al, but higher than that for AISI-316L type stainless steel. When the NiAl intermetallic alloy was heat treated at 400 °C during 144 h or alloyed with Li, the corrosion rate is increased, but this thermal annealing did not affect the corrosion rate of Ni_3Al. This was because by adding Li the adhesion of the external protective layer decrease by inducing a higher number of discontinuities with a higher number of grain boundaries. When the alloys were thermally annealed, these grain boundaries disappeared, decreasing the number of paths for the outwards diffusion of Al from the alloy to form the external, protective Al_2O_3 layer.

Acknowledgement

The authors want to thank to R. Guardian for technical assistance in the SEM images.

References

[1] J.P.P. Huijsmans, G.J. Kraaij, R.C. Makkus, G. Rietveld, E.F. Sitters, J. Power Sources 86 (2000) 117–121.
[2] A. Dicks, A. Siddle, J. Power Sources 86 (2000) 316–323.
[3] K. Tanimoto, M. Yanagida, T. Kojima, J. Power Sources 72 (1998) 77–80.
[4] J.E. Indacochea, I. Bloom, M. Krumpelt, J. Mater. Res. 13 (1998) 7–12.
[5] M. Murai, K. Takisawa, K. Soejima, H. Sotouchi, J. Electrochem. Soc. 143 (1996) 11–16.
[6] F.J. Pérez, D. Duday, M.P. Hierro, Surf. Coat. Technol. 161 (2002) 293–301.
[7] A. Agüero, F.J. García de Blas, M.C. García, Surf. Coat. Technol. 146 (2001) 578–585.
[8] M.J. Escudero, T. Rodrigo, J. Soler, J. Power Sources 118 (2003) 23–24.
[9] P.F. Tortorelli, P.S. Bishop, in: R.H. Jones, R.E. Ricker (Eds.), Environmental Effects on Advanced Materials, The Minerals, Metals and Materials Society, Warrendale, PA, 1991, pp. 91–96.
[10] P.F. Tortorelli, K. Natesan, Mater. Sci. Eng. A258 (1998) 115–125.
[11] M. Salazar, A. Albiter, G. Rosas, R. Perez, Mater. Sci. Eng. 351A (2003) 154–156.
[12] J.P.T. Vossen, R.C. Markus, J. Electrochem. Soc. 143 (1996) 66–71.
[13] M.W. Brumm, H.J. Grabke, B. Wagemann, Corros. Sci. 36 (1994) 37–53.
[14] I. Uchida, T. Nishina, Y. Mugikura, K. Itaya, J. Electroanal. Chem. 206 (1986) 229–235.
[15] T. Nishina, I. Uchida, Proceedings of the Symposium on Molten Carbonate Fuel Cell Technology, vol. pv90-16, The Electrochemical Society, 1990, pp. 438–444.
[16] R.A. Donado, L.G. Marianowski, H.C. Maru, J.R. Selman, J. Electrochem. Soc. 131 (1984) 2535–2541.
[17] H.S. Hsu, J.H. Devan, J. Electrochem. Soc. 133 (1986) 2077–2082.
[18] X. Songbo, Z. Yongda, H. Xing, Z. Bangna, Y. Zhongxing, J. Power Sources. 103 (2002) 230–236.
[19] S. Frangini, A. Masci, Surf. Coat. Technol. 184 (2004) 31–36.